RESEARCH ARTICLE

Oil-soluble polymer brushes-functionalized nanoMOFs for highly efficient friction and wear reduction

Jianxi LIU[1],*, **Yong QIAN**[1], **Dongsheng LI**[2], **Wei WU**[1], **Mengchen ZHANG**[1], **Jie YAN**[3], **Bin LI**[3], **Feng ZHOU**[3]

[1] *State Key Laboratory of Solidification Processing, Center of Advanced Lubrication and Seal Materials, School of Materials Science and Engineering, Northwestern Polytechnical University, Xi'an 710072, China*

[2] *Shaanxi Engineering Research Center of Special Sealing Technology, Xi'an Aerospace Propulsion Institute, Xi'an 710100, China*

[3] *State Key Laboratory of Solid Lubrication, Lanzhou Institute of Chemical Physics, Chinese Academy of Sciences, Lanzhou 730000, China*

Abstract: Nanomaterials as lubricating oil additives have attracted significant attention because of their designable composition and structure, suitable mechanical property, and tunable surface functionalities. However, the poor compatibility between nanomaterials and base oil limits their further applications. In this work, we demonstrated oil-soluble poly (lauryl methacrylate) (PLMA) brushes-grafted metal-organic frameworks nanoparticles (nanoMOFs) as lubricating oil additives that can achieve efficient friction reduction and anti-wear performance. Macroinitiators were synthesized by free-radical polymerization, which was coordinatively grafted onto the surface of the UiO-67 nanoparticles. Then, PLMA brushes were grown on the macroinitiator-modified UiO-67 by surface-initiated atom transfer radical polymerization, which greatly improved the lipophilic property of the UiO-67 nanoparticles and significantly enhanced the colloidal stability and long-term dispersity in both non-polar solvent and base oil. By adding UiO-67@PLMA nanoparticles into the 500 SN base oil, coefficient of friction and wear volume reductions of 45.3% and 75.5% were achieved due to their excellent mechanical properties and oil dispersibility. Moreover, the load-carrying capacity of 500 SN was greatly increased from 100 to 500 N by the UiO-67@PLMA additives, and their excellent tribological performance was demonstrated even at a high friction frequency of 65 Hz and high temperature of 120 °C. Our work highlights oil-soluble polymer brushes-functionalized nanoMOFs for highly efficient lubricating additives.

Keywords: MOFs; polymer brushes; surface modification; tribological properties; friction reduction; anti-wear

1 Introduction

Energy dissipation caused by industrial friction and wear was the leading cause of unnecessary energy consumption, economic losses, and greenhouse gas emissions, which exhausted globally 103 EJ of energy, 250,000 million Euro, and produced 8,120 million tons of CO_2 [1, 2]. Lubrication oils are essential in reducing friction and wear, consisting of base oil and functional additives (such as anti-friction or wear [3, 4], anti-oxidation [5], and extreme-pressure reagents [6]). Traditional lubricating oil additives are mainly organic compounds, such as ionic liquids [7], sulfurized olefins [6], zinc dialkyldithiophosphate [8, 9], and dialkyldithiophosphate (DDP) [10], which could potentially lead to environmental pollution and corrosion of metal. Further, nanomaterials have attracted gradual interest as lubricating oil additives for polishing, mending, and rolling of nanospheres and tribochemical protective film [11–13]. Different types of nanomaterials have been applied in lubricants, such as graphene [14], boron nitride [15], MoS_2 [16, 17], Cu [18], carbon [19], ZnO_2 [20], and SiO_2 [21]. However, the poor compatibility of these inorganic materials

* Corresponding author: Jianxi LIU, E-mail: jianxiliu@nwpu.edu.cn

with base oils are still a significant challenge to meet the requirements of advanced lubricating oil.

As hybrid material, metal-organic framework nanoparticles (nanoMOFs) consist of inorganic metal ions or clusters and organic ligands, which are coordinately bonded to form porous nanomaterials [22]. Unlike conventional lubricant additives, the highly designable organic ligand and tunable surface functionalities of nanoMOFs [23–25] can enhance compatibility with lubricants. Reports have demonstrated that small-size zeolitic imidazolate frameworks-8 (ZIF-8) nanoparticles can contribute to lubrication enhancement [26], and DDP-functionalized Zr-MOFs can achieve friction and wear reduction as well as anti-oxidation [5]. However, ZIF-8 nanoparticles are unstable in an acidic environment, and the high van der Waals attraction between DDP-functionalized nanoMOFs results in quick precipitation in non-polar oils.

Compared to the small molecules, polyelectrolyte brushes functionalized nanoMOFs can greatly enhance their aqueous stability, dispersity, and lubricating performance [27]. In addition, surface-grafted oil-soluble polymer brushes with long-chain alkyl can effectively enhance the dispersity of nanoparticles in base oil owing to the similar chemical composition and highly swollen structure in good solvents [28, 29]. Wright et al. [30] reported the oil-soluble brush grafted on silica nanoparticles. These hybrid nanoparticles exhibit outstanding dispersibility and superior stability in non-polar or low-polar solvents [31] because of the solvation forces from the favourable enthalpic interactions and the entropic and steric repulsions between hairy nanoparticles, effectively preventing nanoparticles from aggregation [32].

Here we show oil-soluble poly (lauryl methacrylate) (PLMA) brushes-functionalized nanoMOFs that can achieve highly efficient friction reduction and anti-wear performance in oil. As an organic–inorganic hybrid material, UiO-67 nanoparticles were synthesized by the solvothermal method. For surface modification, the macroinitiator of P(MAA-co-HEMBr) was fabricated by free-radical copolymerization, which was then grafted onto the surface of the UiO-67 nanoparticles. Then, PLMA brushes were grown on the macroinitiator-modified UiO-67 via a surface-initiated atom transfer radical polymerization (SI-ATRP) strategy. After surface

modification, the compatibility and dispersity of the UiO-67 nanoparticles in a non-polar solvent and base oil were significantly improved. Friction tests demonstrated that both coefficients of friction and wear volume of 500 SN base oil decreased by over 50% after the addition of the UiO-67@PLMA, which showed high load-carrying capacity and durability even at the high frequency of 65 Hz and high temperature of 120 °C.

2 Results and discussion

2.1 Growth of PLMA brushes on nanoMOFs

Scheme 1 depicts the growth of the PLMA brushes on the surface of MOFs nanoparticles to construct a MOFs@PLMA hybrid. UiO-67 nanoparticles formed by zirconium clusters and rigid organic joints exhibited good mechanical stability due to their stronger coordination bond and high connectivity [5, 33]. In this work, P(MAA-co-HEMBr) macroinitiators were synthesized by free-radical copolymerization and trifluoroacetic acid (TFA) acidification treatment, which was then assembled onto the surface of the UiO-67 via the coordination interaction between the carboxylic acid of macroinitiator and the coordinatively unsaturated zirconium cluster sites [34]. Then, PLMA brushes were grown on the surface of the macroinitiator-modified Zr-MOFs via SI-ATRP reaction catalyzed by N,N,N',N',N''-pentamethyldiethylenetriamine (PMDETA) and CuBr complex.

Figure 1 shows the scanning electron microscopy (SEM) and transmission electron microscopy (TEM) images of the UiO-67 nanoparticles before and after polymer brushes modification, which were prepared by drop-casting petroleum ether solution of the samples onto the silicon wafer and ultra-thin carbon film. The average size of the as-synthesized UiO-67 was about (82.1 ± 25) nm, which showed a heavy aggregation phenomenon because of the high surface energy of nanoMOFs (Figs. 1(a) and 1(d)). After grafting the macroinitiator, no obvious change was observed in the UiO-67@Macroinitiator in shape and size compared with the UiO-67 (Figs. 1(b) and 1(e)). A similar agglomeration problem was observed from the UiO-67@Macroinitiator due to its poor dispersity. Notably, great separation of the UiO-67@PLMA
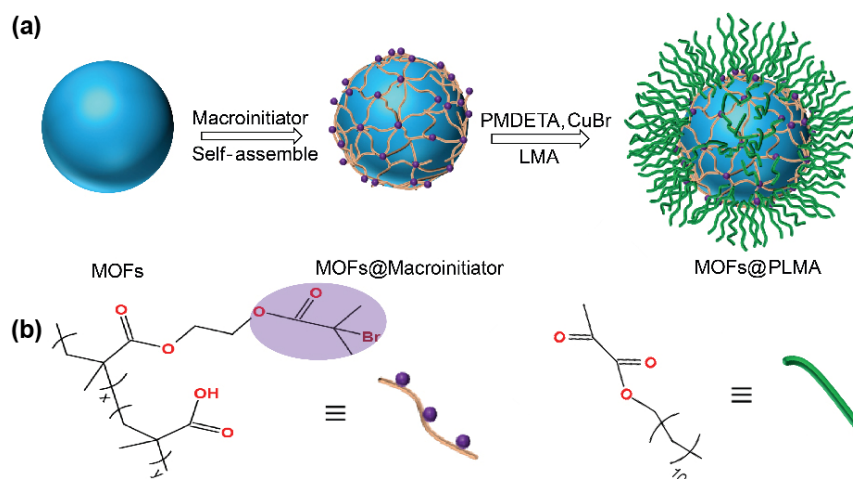
Scheme 1 Schematic diagram of PLMA brushes growth on MOFs nanoparticles. (a) Experimental procedures. (b) Molecular structure of macroinitiator and monomer of LMA.
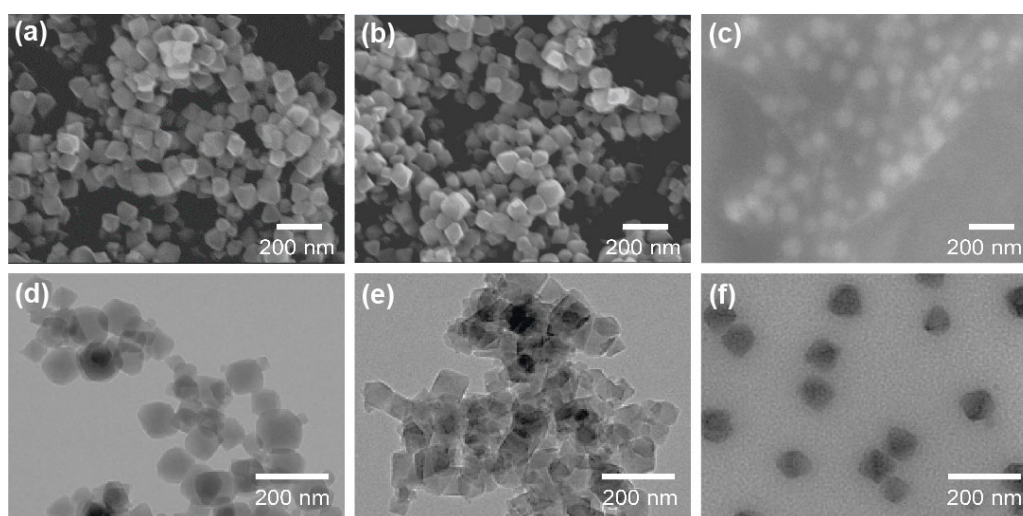

Fig. 1 Size and shape of UiO-67 nanoparticles maintained after grafting PLMA. (a–c) SEM and (d–f) TEM images of the (a, d) UiO-67, (b, e) UiO-67@Macroinitiator and (c, f) UiO-67@PLMA nanoparticles.

nanoparticles appeared on the images, while no noticeable change was demonstrated for their shape and size (Figs. 1(c) and 1(f)). The corresponding TEM energy dispersive spectrometer mapping of the UiO-67@PLMA showed that oxygen and zirconium were evenly distributed, as well as the less abundant bromine (Fig. S1 the Electronic Supplementary Material (ESM)). These results showed that PLMA brushes significantly improved the aggregation phenomenon of UiO-67 in a non-polar solvent.

2.2 Physicochemical properties of the UiO-67@PLMA nanoparticles

To investigate the chemical structure of the UiO-67@PLMA, we conducted infrared (IR) and thermogravimetric (TG) measurements of the UiO-67 nanoparticles with and without polymer brushes functionalization. IR spectra of the UiO-67@Macroinitiator showed the appearance of a stretching vibration peak of the C=O bond at 1,725 cm^{-1} (Fig. 2(a)), indicating the assembly of macroinitiator on the UiO-67 nanoparticle surface [28]. After growing the PLMA brushes, the IR spectrum of the UiO-67@PLMA appeared the symmetry and asymmetric stretch vibration of the C–H bond at 2,854 cm^{-1} and 2,920 cm^{-1}, which indicated the successful growth of the polymer brushes [35]. The X-ray photoelectron spectroscopy (XPS) spectra of UiO-67@Macroinitiator showed that
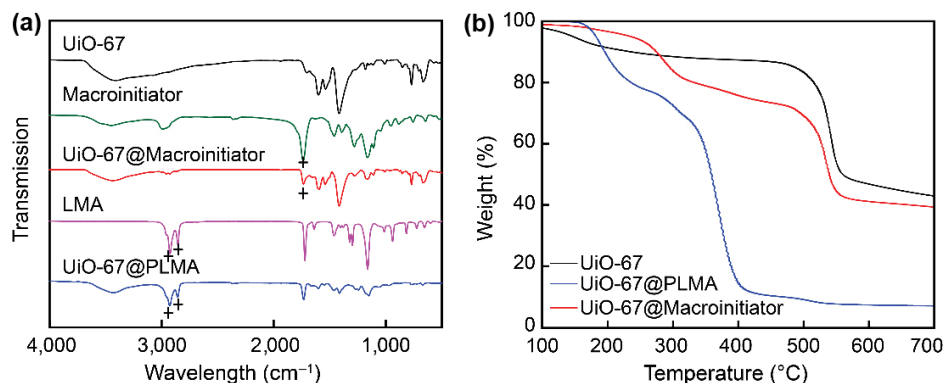
Fig. 2 Growth of PLMA polymer brush on the UiO-67 nanoparticles. (a) FTIR spectrum of the UiO-67 with and without appearance of PLMA. (b) TG curves of the UiO-67 before and after grafting PLMA.

the characteristic peaks of Br 3d at 68.7 eV appeared to compare with the UiO-67, which were not present in the spectra of UiO-67. Notable, the intensity of Zr 3d at 180.2 eV greatly reduced after the PLMA growth (Fig. S2 in the ESM). Calculating the retained quantity of samples in TG curves at 700 °C demonstrated that 7.5 wt% macroinitiators and 34.1 wt% PLMA brushes were modified onto the UiO-67 nanoparticles, respectively (Fig. 2(b)).

Figure 3(a) shows the X-ray diffractometer (XRD)

pattern of the UiO-67 with and without modification of PLMA brushes. The crystallinity of UiO-67@PLMA showed uniformity similar to that of both the as-synthesized and simulated UiO-67, which indicated that the crystallinity and phase purity were retained. To measure the surface wettability of the samples, we pressed UiO-67 and UiO-67@PLMA powder into lumps by tablet press. The contact angle of the UiO-67 was 47.8°, indicating the material surface's hydrophilicity. In contrast, the UiO-67@PLMA increased to 126.6°
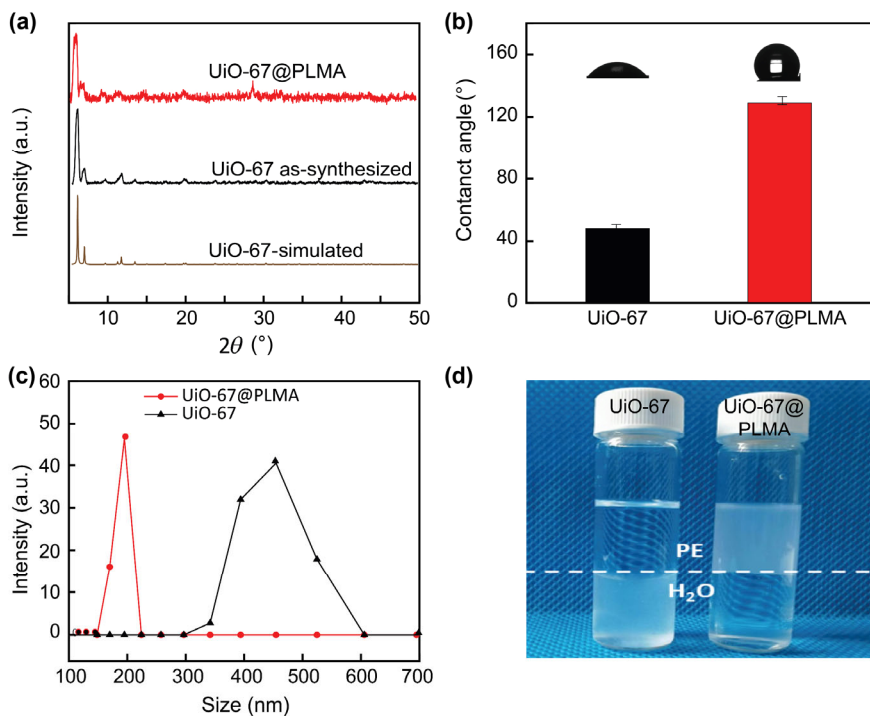

Fig. 3 Characterization of physical and chemical properties of the PLMA functionalzied MOFs. (a) PXRD patterns of the UiO-67 and UiO-67@PLMA. (b) Static water contact angle of the UiO-67 and UiO-67@PLMA. (c) Hydrodynamic diameter distribution of the UiO-67 and UiO-67@PLMA suspended in PE. (d) Photograph of the UiO-67 (left) and UiO-67@PLMA (right) dispersed in a mixture of deionized water and petroleum ether after shaking.

because of the hydrophobicity of the long alkanes in PLMA polymer brushes [36] (Fig. 3(b)). The hydrodynamic size distribution peak of the UiO-67 nanoparticles suspended in PE was 459 nm, and this value shifted to 190 nm for UiO-67@PLMA, which indicated that the dispersity of the UiO-67 in non-polar organic solvents was greatly enhanced (Fig. 3(c)). UiO-67 nanoparticles quickly aggregated and settled in deionized water due to their high surface energy when dispersed in a mixture of petroleum and water. Conversely, UiO-67@PLMA nanoparticles remained stably dispersed in the mixture even after strong shaking, which attributed to the reduced surface energy and enhanced compatibility of UiO-67 after surface modification. Thus, the above results indicated that the polymer brushes successfully grafted onto the UiO-67, which improved the surface hydrophobicity of the UiO-67 nanoparticles to enhance their dispersity in non-polar solvents.

2.3 Dispersity of the UiO-67@PLMA in base oil

To investigate the influence of the modification of PLMA brushes on the dispersity of UiO-67 nanoparticles in base oil, we conducted static precipitation experiments of the UiO-67 before and after grafting the PLMA brush at different temperatures. Figure 4 depicts the long-term dispersion stability of 0.6 wt% UiO-67
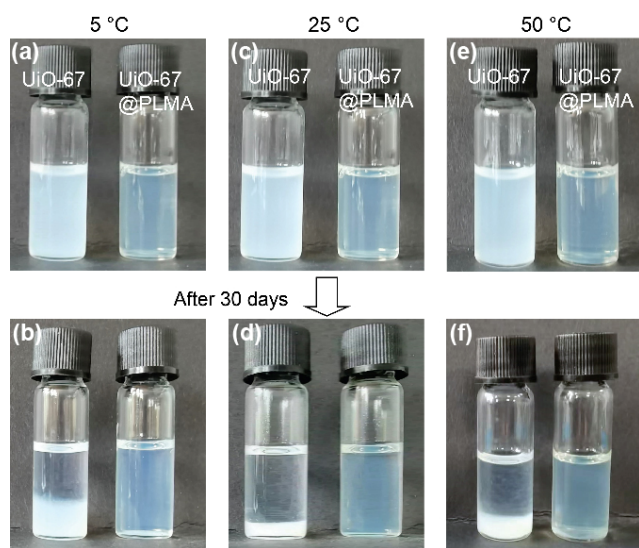

Fig. 4 Long-term dispersity of the UiO-67@PLMA nanoparticles in base. Optical images of 0.6 wt% suspension of the UiO-67 (left) and the UiO-67@PLMA (right) in 500SN in the initial state (a, c, e) at 5, 25, 50 °C and after being keep for 30 days (b, d, f).

and UiO-67@PLMA in 500 SN from 1 to 30 days at 5, 25, and 50 °C, respectively. The UiO-67@PLMA oil suspension showed a clearer solution at various temperatures. After keeping for 30 days, the UiO-67 completely settled at the bottom of the bottle, indicating the UiO-67 could not be dispersed at 500 SN for a long time at 5 °C. In contrast, UiO-67@PLMA suspension dispersed stability and existed no significant change in transparency because of the enthalpic interactions between PLMA brushes and 500 SN and the entropic steric repulsions of UiO-67@PLMA [30]. Similarly, the suspension stayed clear, and no change in transparency was observed after 30 days at 25 and 50 °C, demonstrating the superior stability of the UiO-67@PLMA in 500 SN. Thus, the functionalization of MOFs with PLMA brushes greatly enhanced compatibility between the UiO-67 nanoparticles and base oil, and the UiO-67@PLMA additives possessed long-term dispersion stability.

2.4 Tribological properties of the UiO-67@PLMA as additives in base oil

Figure 5 compares the tribological property of the UiO-67 additives before and after growing the PLMA brushes in 500 SN base oil. On the SRV-V friction motor, the bearing steel was used as the friction pair, and the typical disc contact method was used to perform the friction test of the functionalized MOFs as additives in the oil. COF of the pure 500 SN started at the value below 0.15 but quickly increased to above 0.2 because of the occurrence of scuffing (Fig. 5(a) and Fig. S3 in the ESM), which decreased gradually and stabilized finally at 0.203. The coefficient of friction (COF) of the UiO-67 with 0.6 wt% addition in base oil reached above 0.2 in the running-in stage and gradually decreased and stabilized at 0.165. After macroinitiator modification, the COF with 0.6 wt% UiO-67@Macroinitiator added to 500 SN reached 0.27 during the running-in period, then decreased and stabilized at 0.20. For the UiO-67@PLMA nanoparticles, adding 0.6 wt% in 500 SN significantly improved the lubricating performance, and the COF was stable at 0.111 and lower than that of 500 SN over the whole reciprocating experiment.

For the wear volume on the bearing steel disks, the 500 SN reached the value of 1.65×10^5 μm³,
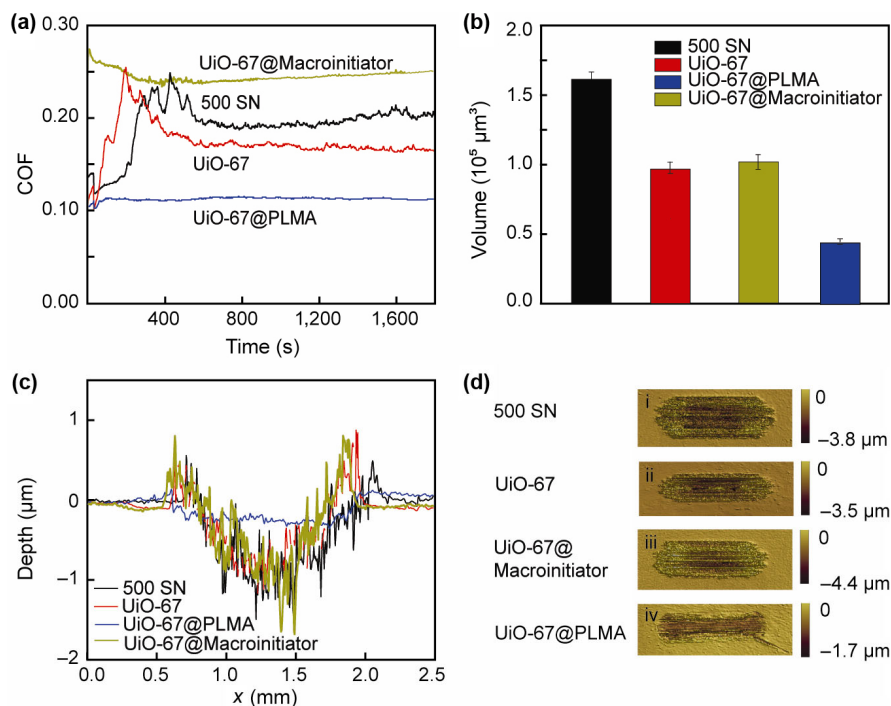
Fig. 5 Tribological properties of the UiO-67@PLMA additives in oil. (a) COF, (b)wear volume, and (c) cross-sectional profiles of worn scars in the *x*-axis direction of the 0.6 wt% UiO-67 and UiO-67@PLMA as 500 SN additives. (d) Worn scar of UiO-67 nanoparticles as 500 SN (i), UiO-67 (ii), UiO-67@Macroinitiator (iii) and UiO-67@PLMA (iv) (normal load: 100 N, temperature: 50 °C, frequency: 25 Hz, stroke: 1 mm).

which reduced to 0.98×10^5 μm^3 after the addition of 0.6 wt% of UiO-67 (Fig. 5(b)). After adding UiO-67@Macroinitiator in the base oil, the wear volume value raised to 1.12×10^5 μm^3 due to extremely poor dispersion in the base oil. Notably, the wear volume of UiO-67@PLMA-based lubricant was significantly reduced to 4.18×10^4 μm^3, which decreased by 75.5% compared with 500 SN. Meanwhile, 500 SN oil had a very wide and rough worn scar with many grooves on the bearing steel disks, which showed a wear depth of 1.29 μm (Figs. 5(c) and 5(d)). After adding the UiO-67, the depth of the scar (1.02 μm) was slightly shallower than the base oil. The wear depth of UiO-67@Macroinitiator raised to 1.35 μm. In comparison, adding the UiO-67@PLMA in oil made the scar the shallowest, and the wear depth decreased from 1.35 to 0.23 μm. Therefore, modifying UiO-67 with PLMA greatly improved the tribological properties as oil additives.

To reveal the relationship between the COF and the addition concentration, we investigated tribological properties of the UiO-67@PLMA additives from 0.2 wt% to 1.0 wt% at 100N, 50 °C, 25 Hz. As depicted

in Fig. 6(a), the coefficient of friction for 500 SN increased rapidly to 0.25 after 190 s, which gradually decreased to 0.205. After adding 0.2 wt% of the UiO-67@PLMA, the coefficient of friction curve showed a slight delay in lubrication failure time compared to pure 500 SN, which eventually reduced to 0.201. When the addition amount was increased to 0.4 wt%, 0.6 wt%, 0.8 wt%, and 1.0 wt%, the curve was stable at a low level throughout. We found that the COF started decreasing with the addition concentration rising and then increased when the concentration exceeded 0.6 wt%. Figure 6(b) shows the wear volumes of the UiO-67@PLMA as oil additives in different concentrations. The wear volume continued to decrease as the addition amount increased from 0.2 wt% to 0.6 wt%, which gradually increased at higher concentrations. The additional amount of 0.6 wt% possessed the best anti-wear performance, and the wear volume was reduced from 1.56×10^5 to 3.87×10^4 μm^3 (~75.19%), indicating the superior anti-wear performance of UiO-67@PLMA. Furthermore, using the UiO-67@PLMA as an oil additive significantly reduced the width of the worn scar (Figs. 6(c) and
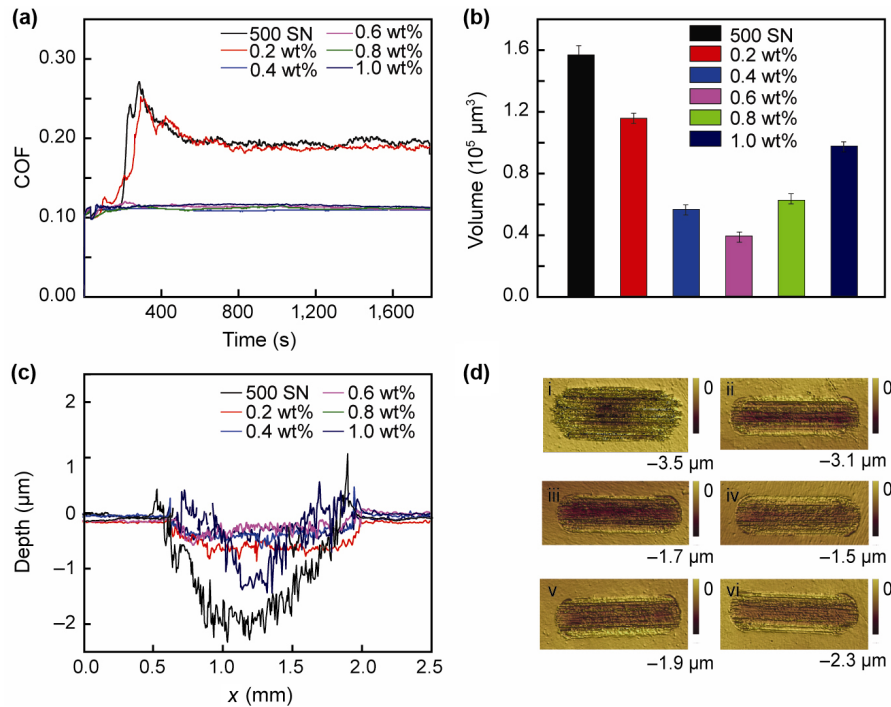
Fig. 6 Concentration depedent tribological properties of the UiO-67@PLMA as oil additives. (a) COF, (b) wear volume, and (c) cross-sectional profiles of worn scars in the x-axis direction of the UiO-67@PLMA as 500 SN additives with the amount of addition from 0.2 wt% to 1.0 wt%. (d) Photographs of worn scar of UiO-67 nanoparticles as 500 SN (i),0.2 wt % (ii), 0.4 wt % (iii), 0.6 wt % (iv), 0.8 wt % (v) and 1.0 wt % UiO-67@PLMA.

6(d)). The depth of the worn scar gradually decreased, then increased with increasing the additional concentration. In addition, the 3D profiling image showed that 0.6 wt% addition possessed the lowest worn scar diameter and depth. The friction reduction and anti-wear performance are consistent in the UiO-67@PLMA additives at their best addition concentration.

Figure 7 depicts a comprehensive tribological study of the UiO-67 and UiO-67@PLMA additives in base oil at different friction testing conditions, such as loads, temperatures, and frequencies. Figure 7(a) shows the COF curves of the lubricants with the effect of temperature rise. The COF of the 500 SN was stable at temperatures below 40 °C, but it increased sharply to about 0.26 at 50 °C. Compared to 500 SN, the lubrication failure temperature increased from 40 to 70 °C with the addition of the UiO-67. For the 500 SN added with UiO-67@PLMA, the COF value kept stable at a low level throughout the process, indicating a significant improvement in the temperature-bearing capacity. To further compare the tribological properties of the different lubricants, COF curves were tested by

ramping frequency from 10 to 65 Hz with stepping load of 5 Hz (Fig. 7(b)). Lubrication failure of the 500 SN and that added with UiO-67 appeared at 15 and 25 Hz, respectively. After adding 0.6 wt% UiO-67@PLMA, the failure was inhibited and showed a stable and low COF of 0.11. Figure 7(c) shows the load-carrying capacity performance of the different samples. The load-carrying capacity of UiO-67 lubricating oil can be increased from 100 to 300 N. In contrast, the maximum load capacity reached 500 N after adding UiO-67@PLMA. These results indicated that the PLMA functionalized UiO-67 significantly improved the tribological properties of the base oil 500 SN.

In addition, we examined the tribological properties of the UiO-67@PLMA in PAO10 base oil, which also had a good dispersibility. The COF of PAO10 raised rapidly to 0.232 and gradually decreased to around 0.186 (Fig. S4 in the ESM). For the UiO-67@PLMA in PAO10, the COF was stable at 0.115, which significantly improved the lubricating performance of PAO10. For the wear volume onthe bearing steel disks, the PAO10 reached the value of 1.58×10^5 μm^3, which reduced to
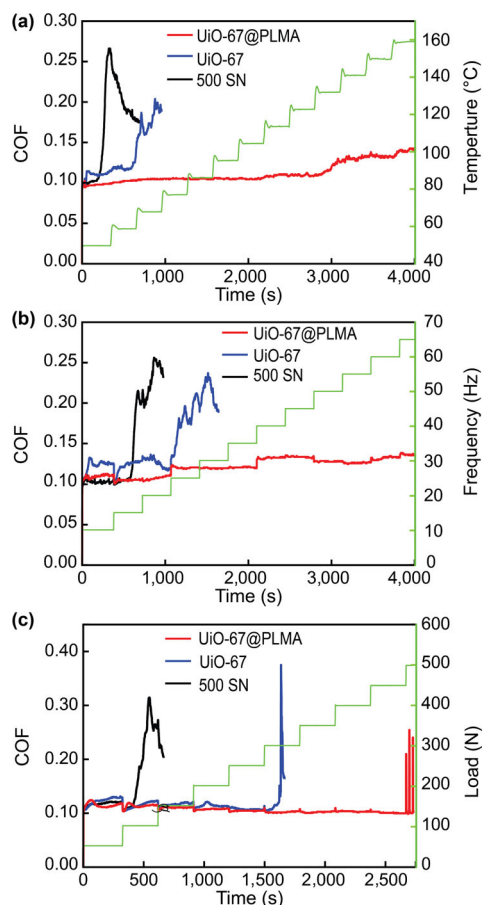
Fig. 7 Comprehensive tribological properties of the lubricating additives with evolution of COF curve for under different conditions. (a) temperature conversion conditions (100 N, 25 Hz, and the temperature ramp test from 50 °C to 160 °C at the rate of 10 °C/5 min), (b) frequency conversion conditions (100 N, 50 °C, and the frequency ramp test from 10 Hz to 65 Hz at the rate of 5 Hz/5 min) and (c) extreme pressure (50 °C, 25 Hz, and the load ramp test from 50 N to 500 N at the rate of 50 N/ 5 min).

0.35×10^5 μm^3 after adding 0.6 wt% of UiO-67@PLMA. Thus, the nanocomposite of UiO-67@PLMA works as a promising additive, which can improve the lubricating performance of base oils.

2.5 Lubricating mechanism analysis

To understand the mechanism of friction-reduction and anti-wear performance, we applied SEM measurement to observe the micromorphology of the wear surface of the steel block (Fig. 8). We observed short-range pits and unevenly distributed asperities on the wear scars (Figs. 8(a) and 8(b)), which were attributed to corrosive wear and fatigue wear, respectively [37]. After adding UiO-67 into 500 SN,

the corresponding SEM images displayed long-range furrows and unevenly distributed asperities on the worn surface (Figs. 8(c) and 8(d)), which were attributed to the abrasive wear and fatigue wear [38]. Using UiO-67@PLMA as additives, we found shallower worn scar depth for the UiO-67@PLMA additives in oil (Figs. 8(e) and 8(f)), which can be attributed to the ball-bearing effect of nanomaterials as additives [39]. These results indicated that the UiO-67@PLMA additive in oil had superior anti-wear performance.

To further explain the tribological behaviour of these lubricants, we measured the XPS on the worn scar of the UiO-67@PLMA as oil additives (Fig. S5 in the ESM). The peaks of Fe 2p at 727.3 eV, 725.2 eV, 720.1 eV, and 712.5 eV can be assigned to Fe_2O_3/FeOOH, which coincide with the O 1s peaks of 532.5 eV and 530.7 eV [3, 40] (Figs. S5(b) and S5(c) in the ESM). However, the signal of zirconium was not found on the worn scar (Fig. S5(d) in the ESM). The XPS result showed that a lubricating boundary layer of Fe_2O_3 and FeOOH reduced the interfacial friction. Based on the above analysis, the mechanism responsible for UiO-67@PLMA to reduce friction and wear can be attributed to the synergic effect of the UiO-67 nanoparticles and PLMA brush (Scheme 2). Firstly, PLMA-grafted UiO-67 nanoparticles inhibited the aggregation of nanoMOFs in the base oil, exerted ball-bearin, and resisted direct contact between the two sliding surfaces. Secondly, forming a chemical protective film further reduced friction and wear. Furthermore, PLMA polymer brushes exhibited excellent lubrication properties [30], which advanced the UiO-67@PLMA additives in oil with good tribological performance.

3 Conclusions

In summary, we investigated the application of hydrophobic UiO-67@PLMA as a lubricating oil additive to achieve highly efficient friction and wear reduction. Macroinitiators of P(MAA-co-HEMBr) were coordinately grafted on the surface of UiO-67 nanoparticles with size controllable at about 82 nm. Then, oil-soluble PLMA polymer brushes were grafted onto the UiO-67 using SI-ATRP. We found the size and crystal structure of UiO-67 nanoparticles
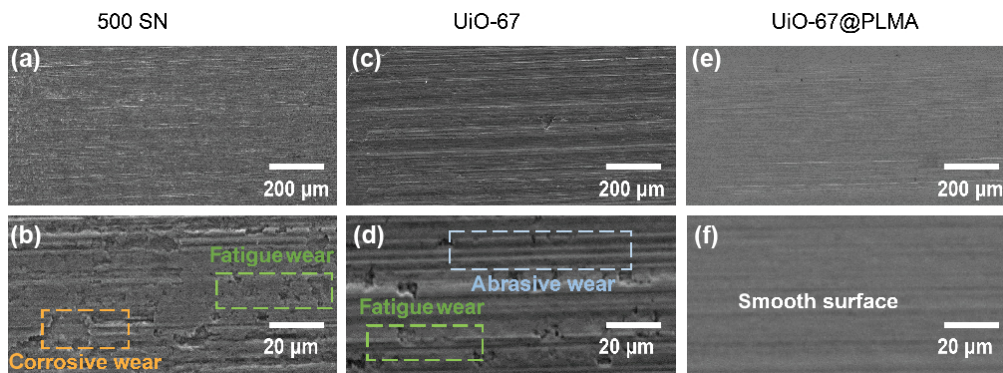
Fig. 8 SEM images of worn surface. Worn scar of the friction test with (a, b) 500 SN, (c, d) UiO-67 and (e, f) UiO-67@PLMA in oil as lubricants under constant conditions (100 N, 50 °C, 25 Hz).
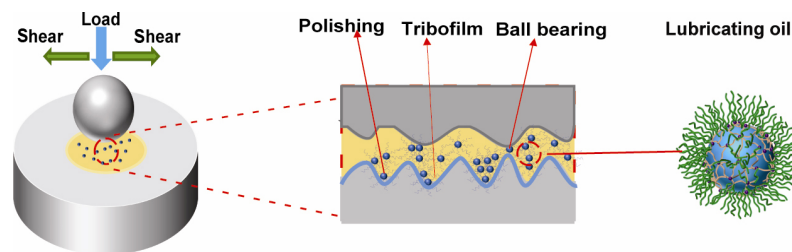
Scheme 2 Lubrication mechanism of the UiO-67@PLMA as additive.

had almost no change upon PLMA growth. The UiO-67@PLMA nanoparticles were well-dispersed in both non-polar solvent and base oil 500 SN, which remained stable for over 30 days at various temperatures of 5, 25, and 50 °C. Long-term friction tests revealed that UiO-67@PLMA additives could reduce friction coefficient by 45.3% and wear volume by over 75.5% as oil additives. Adding 0.6 wt% UiO-67@PLMA increased the load capacity of 500 SN from 100 to 500 N while maintaining stable performance even under variable frequency and temperature conditions. Our oil-soluble polymer brush functionalized nanoMOFs have great potential in improving the tribological properties of lubricants.

4 Experimental

4.1 Preparation and purification of UiO-67 nanoparticles

UiO-67 ($Zr_6O_4(OH)_4(C_{14}H_8O_4)_6$): UiO-67 nanoparticles were synthesized by the solvothermal method using acetic acid as a modulator, which was similar to previously published methods [5]. Biphenyl-4,4'-dicarboxylic acid (2.4 g, 9.6 mmol) was dissolved into

120 mL N, N'-dimethylformamide (DMF) and sonicated for 20 min to generate a homogeneous white suspension. Zirconyl chloride octahydrate (1.08 g, 3.36 mmol) was sonicated into 360 mL DMF to obtain a clear solution. Then, metal ion and organic linker suspensions were mixed into a three-neck flask. Adding 0.5 M acetic acid (13.72 mL) into the solution was sonicated for 5 min and heated at 90 °C for 20 h. After cooling, the synthesized UiO-67 nanoparticles were homogeneously divided into six groups and purified by DMF (3 times) and methanol (3 times) with centrifugation (12,000 rpm, 15 min). Finally, the UiO-67 nanoparticles were re-dispersed into methanol for further use.

4.2 Synthesis of P(MAA-co-HEMBr) macroinitiator

2-(2-Bromoisobutyryloxy)ethyl methacrylate (HEMBr): HEMBr initiator was synthesized by the reported method [41]. HEMA (21.4 mL) and triethylamine (12.0 mL) were typically added into a 250 mL three-necked flask. Then, 70 mL dichloromethane (DCM) was added into the flask, which was kept in an ice bath of 0 °C. After removing oxygen by Ar, 2-Bromoisobutyryl Bromide (19.76 mL) dissolved in DCM (23.1 mL) is dropwise added to the flask. The

reaction proceeded for 4 h at 0 °C. The product was filtered out and rinsed with dichloromethane. The supernatant was washed with saturated Na_2CO_3 and saturated NaCl solution 3 times. An excess amount of anhydrous $MgSO_4$ was added to the solution to remove the water in the rotary evaporator. Finally, a light yellow liquid was harvested for further application.

P(tBuMA-co-HEMBr): P(tBuMA-co-HEMBr) was synthesized according to the previously published method [28]. HEMABr (3.0 g, 10.74 mmol), tert-Butyl methacrylate (tBuMA) (169.4 g, 1.20 mmol), and 2-methyl propionitrile (15.0 mg, 0.09 mmol) were dissolved in 3 mL of DMF in a glass vial. After degassing by argon gas, the vial was heated from 25 to 70 °C and kept for 1 h. The product was obtained by multiple cycles of solvent precipitation in methanol and then dried under a vacuum.

P(MAA-co-HEMBr): P(tBuMA-co-HEMBr) was treated by TFA for 2 h to remove t-butyl groups, and macroinitiator was obtained by multiple cycles of solvent precipitation in methanol and dried under vacuum overnight.

4.3 Synthesis of UiO-67@PLMA nanoparticles

UiO-67@PLMA nanoparticles were prepared by a two-step method. Firstly, 100 mg of UiO-67 and 100 mg of macroinitiator were dispersed into 50 mL DCM. After 20 min sonication, the suspension was stirred for 24 h, which was then centrifuged from the macroinitiator suspension and purified with DCM and toluene. The UiO-67@Macroinitiator nanoparticles were used without drying for UiO-67@PLMA preparation. The UiO-67@Macroinitiator, 6 g LMA, 60 μL PMDETA and 6 mL DMF were added into an ampoule. The nitrogen flow was maintained for 20 min to remove oxygen from the suspension, and then 60 mg CuBr was added into the suspension. The polymerization was performed at 80 °C for 2 h. The UiO-67@PLMA was obtained, and the catalyst and excess monomers were removed by washing with DMF (2 times) and DCM (3 times).

4.4 Characterization

The morphologies of UiO-67, UiO-67@Macroinitiator, and the nanoparticles after grafting PLMA brushes were measured by field-emission scanning electron microscope (FESEM, Zeiss Gemini-500) at an acceleration voltage of 5 kV and field emission transmission electron microscope (FETEM, FEI JEM-F200) at 200 kV, respectively. The chemical structure of the samples was obtained from Fourier transform infrared spectra (FTIR, Bruker Tensor II). The crystallinity was tested from an X-ray diffractometer (XRD, Bruker D8) using CuKα radiation, λ = 1.5404 Å. Surface elemental compositions of the samples and the worn scars were performed by X-ray photoelectron spectroscopy (PHI 5000 VersaProbe III). Thermogravimetric analysis (TG) measurement was tested in Mettler Toledo, with the temperature measurement range of 100−700 °C (10 °C/min). The tribological performance of the samples was performed by high-frequency linear friction and wear testing machine (SRV-V) and 3D surface profiler (Bruker, GTK-18–0433).

Declaration of competing interest

The authors have no competing interests to declare that are relevant to the content of this article. The author Feng ZHOU is the Editorial Board Member of this journal.

Electronic Supplementary Material Supplementary material is available in the online version of this article at https://doi.org/10.1007/s40544-023-0823-x.

The images or other third party material in this article are included in the article's Creative Commons licence, unless indicated otherwise in a credit line to the material. If material is not included in the article's Creative Commons licence and your intended use is not permitted by statutory regulation or exceeds the permitted use, you will need to obtain permission directly from the copyright holder.

To view a copy of this licence, visit http://creativecommons.org/licenses/by/4.0/.

References

[1] Holmberg K, Erdemir A. Influence of tribology on global energy consumption, costs and emissions. *Friction* **5**(3): 263–284 (2017)

[2] Holmberg K, Kivikytö-Reponen P, Härkisaari P, Valtonen K, Erdemir A. Global energy consumption due to friction and wear in the mining industry. *Tribol Int* **115**: 116–139 (2017)

[3] Ye Q, Liu S, Xu F, Zhang J, Liu S J, Liu W M. Nitrogen-phosphorus codoped carbon nanospheres as lubricant additives for antiwear and friction reduction. *ACS Appl Nano Mater* **3**(6): 5362–5371 (2020)

[4] Liu J X, Luo H W, Qian Y, Li F, Wu W, X. Yi X B, Shi J Q, Tian Y L, Zhang S M. DDP-functionalized UiO-67 nano-particles as lubricating oil additives for friction and wear reduction. *Tribol Int*. **186**: 108627(2023)

[5] Wu W, Liu J X, Li Z H, Zhao X Y, Liu G Q, Liu S J, Ma S H, Li W M, Liu W M. Surface-functionalized nanoMOFs in oil for friction and wear reduction and antioxidation. *Chem Eng J* **410**: 128306 (2021)

[6] Niu W X, Yuan M, Wang P F, Shi Q, Xu H, Dong J X. One-pot synthesis of SIB@ZIF-8 with enhanced anti-corrosion properties and excellent lubrication properties. *Tribol Int* **151**: 106491 (2020)

[7] Yu Q L, Wang Y R, Huang G W, Ma Z F, Shi Y J, Cai M R, Zhou F, Liu W M. Task-specific oil-miscible ionic liquids lubricate steel/light metal alloy: A tribochemistry study. *Adv Materials Inter* **5**(19): 1800791 (2018)

[8] Yang S Y, Zhang D T, Wong J S S, Cai M R. Interactions between ZDDP and an oil-soluble ionic liquid additive. *Tribol Int* **158**: 106938 (2021)

[9] Lei X, Zhang Y J, Zhang S M, Yang G B, Zhang C L, Zhang P Y. Study on the mechanism of rapid formation of ultra-thick tribofilm by CeO₂ nano additive and ZDDP. *Friction* **11**(1): 48–63 (2023)

[10] Dorgham A, Parsaeian P, Azam A, Wang C, Ignatyev K, Mosselmans F, Morina A, Neville A. Tribochemistry evolution of DDP tribofilms over time using *in situ* synchrotron XAS.

Tribol Int **160**: 107026 (2021)

[11] Dai W, Kheireddin B, Gao H, Liang H. Roles of nanoparticles in oil lubrication. *Tribol Int* **102**: 88–98 (2016)

[12] Waqas M, Zahid R, Bhutta M U, Khan Z A, Saeed A. A review of friction performance of lubricants with nano additives. *Materials* **14**(21): 6310 (2021)

[13] Zhang X Z, Lu Q, Yan Y J, Zhang T T, Liu S J, Cai M R, Ye Q, Zhou F, Liu W M. Tribochemical synthesis of functionalized covalent organic frameworks for anti-wear and friction reduction. *Friction* **11**(10): 1804–1814 (2023)

[14] Kong S, Wang J B, Hu W J, Li J S. Effects of thickness and particle size on tribological properties of graphene as lubricant additive. *Tribol Lett* **68**(4): 1–10 (2020)

[15] Fan X Q, Gan C L, Feng P, Ma X L, Yue Z F, Li H, Li W, Zhu M H. Controllable preparation of fluorinated boron nitride nanosheets for excellent tribological behaviors. *Chem Eng J* **431**: 133482 (2022)

[16] Guo J D, Peng R L, Du H, Shen Y B, Li Y, Li J H, Dong G N. The application of nano-MoS₂ quantum dots as liquid lubricant additive for tribological behavior improvement. *Nanomaterials* **10**(2): 200 (2020)

[17] Guo J L, Zeng C, Wu P X, Liu G Q, Zhou F, Liu W M. Surface-functionalized Ti₃C₂Tₓ MXene as a kind of efficient lubricating additive for supramolecular gel. *ACS Appl Mater Interfaces* **14**(46): 52566–52573 (2022)

[18] Yang G B, Zhang Z M, Zhang S M, Yu L G, Zhang P Y. Synthesis and characterization of highly stable dispersions of copper nanoparticles by a novel one-pot method. *Mater Res Bull* **48**(4): 1716–1719 (2013)

[19] He J Q, Sun J L, Choi J, Wang C L, Su D X. Synthesis of N-doped carbon quantum dots as lubricant additive to enhance the tribological behavior of MoS₂ nanofluid. *Friction* **11**(3): 441–459 (2023)

[20] Wu L L, Zhang Y J, Yang G B, Zhang S M, Yu L G, Zhang P Y. Tribological properties of oleic acid-modified zinc oxide nanoparticles as the lubricant additive in poly-alpha olefin and diisooctyl sebacate base oils. *RSC Adv* **6**(74): 69836–69844 (2016)

[21] Gao K, Chang Q Y, Wang B, Zhou N N, Qing T. The purification and tribological property of the synthetic magnesium silicate hydroxide modified by oleic acid. *Lubr Sci* **30**(7): 377–385 (2018)

[22] Wang S Z, McGuirk C M, D'Aquino A, Mason J A, Mirkin C A. Metal–organic framework nanoparticles. *Adv Mater* **30**(37): e1800202 (2018)

[23] Lu W G, Wei Z W, Gu Z Y, Liu T F, Park J, Park J, Tian J, Zhang M W, Zhang Q, Gentle T, *et al*. Tuning the structure and function of metal–organic frameworks via linker design. *Chem Soc Rev* **43**(16): 5561–5593 (2014)

[24] Wu W, Liu J X, Gong P W, Li Z H, Ke C, Qian Y, Luo H W, Xiao L S, Zhou F, Liu W M. Construction of core-shell NanoMOFs@microgel for aqueous lubrication and thermal-responsive drug release. *Small* **18**(28): e2202510 (2022)

[25] Wu W, Liu J X, Lin X, He Z Z, Zhang H, Ji L, Gong P W, Zhou F, Liu W M. Dual-functional MOFs-based hybrid microgel advances aqueous lubrication and anti-inflammation. *J Colloid Interface Sci* **644**: 200–210 (2023)

[26] Bowman W F, Stachowiak G W. The effect of base oil oxidation on scuffing. *Tribol Lett* **4**(1): 59–66 (1998)

[27] Wu W, Liu J X, Tian L J, Lin X, Xue H D, Gong P W, Zhou F, Liu W M. Polyelectrolyte-functionalized NanoMOFs for highly efficient aqueous lubrication and sustained drug release. *Macromol Rapid Commun* **44**(13): e2300089 (2023)

[28] He S F, Wang H L, Zhang C Z, Zhang S W, Yu Y, Lee Y J, Li T. A generalizable method for the construction of MOF@polymer functional composites through surface-initiated atom transfer radical polymerization. *Chem Sci* **10**(6): 1816–1822 (2019)

[29] He M R, Sun Y L, Tan X L, Luo J, Zhang H Y. Bioinspired oil-soluble polymers based on catecholamine chemistry for reduced friction. *J Appl Polym Sci* **138**(21): 50472 (2021)

[30] Wright R A E, Wang K W, Qu J, Zhao B. Oil-soluble polymer brush grafted nanoparticles as effective lubricant additives for friction and wear reduction. *Angew Chem Int Ed* **55**(30): 8656–8660 (2016)

[31] Li D J, Sheng X, Zhao B. Environmentally responsive "hairy" nanoparticles: mixed homopolymer brushes on silica nanoparticles synthesized by living radical polymerization techniques. *J Am Chem Soc* **127**(17): 6248–6256 (2005)

[32] Seymour B T, Wright R A E, Parrott A C, Gao H Y, Martini A, Qu J, Dai S, Zhao B. Poly(alkyl methacrylate) brush-grafted silica nanoparticles as oil lubricant additives: Effects of alkyl pendant groups on oil dispersibility, stability, and lubrication property. *ACS Appl Mater Interfaces* **9**(29): 25038–25048 (2017)

[33] Cavka J H, Jakobsen S, Olsbye U, Guillou N, Lamberti C, Bordiga S, Lillerud K P. A new zirconium inorganic building brick forming metal organic frameworks with exceptional stability. *J Am Chem Soc* **130**(42): 13850–13851 (2008)

[34] Zhu W, Xiang G L, Shang J, Guo J M, Motevalli B, Durfee P, Agola J O, Coker E N, Brinker C J. Versatile surface functionalization of metal–organic frameworks through direct metal coordination with a phenolic lipid enables diverse applications. *Adv Funct Materials* **28**(16): 1705274 (2018)

[35] Wu M, Wu M, Pan M, Jiang F, Hui B, Zhou L. Synthesization and characterization of lignin-graft-poly (lauryl methacrylate) via ARGET ATRP. *Int J Biol Macromol* **207**: 522–530 (2022)

[36] Singh H, Sharma S. Hydration of linear alkanes is governed by the small length-scale hydrophobic effect. *J Chem Theory Comput* **18**(6): 3805–3813 (2022)

[37] Lu Q, Zhang T T, He B L, Xu F, Liu S J, Ye Q, Zhou F. Enhanced lubricity and anti-wear performance of zwitterionic polymer-modified N-enriched porous carbon nanosheets as water-based lubricant additive. *Tribol Int* **167**: 107421 (2022)

[38] Meng Y G, Xu J, Jin Z M, Prakash B, Hu Y Z. A review of recent advances in tribology. *Friction* **8**(2): 221–300 (2020)

[39] Wu Y Y, Tsui W C, Liu T C. Experimental analysis of tribological properties of lubricating oils with nanoparticle additives. *Wear* **262**(7–8): 819–825 (2007)

[40] Y. Wang, T. Zhang, Y. Qiu, R. Guo, F. Xu, S. Liu, Q. Ye and F. Zhou. Nitrogen-doped porous carbon nanospheres derived from hyper-crosslinked polystyrene as lubricant additives for friction and wear reduction. *Tribol Int*. **169**: 107458(2022)

[41] Liu G Q, Feng Y, Gao X H, Chen Z, Zhao N, Zhou F, Liu W M. Synovial fluid-inspired biomimetic lubricating microspheres: Zwitterionic polyelectrolyte brushes-grafted microgels. *Friction* **11**(6): 938–948 (2023)

Jianxi LIU. He is currently a professor at Northwestern Polytechnical University, China. He obtained his Ph.D. degree from Karlsruhe Institute of Technology, Germany, in 2015. He performed postdoctoral research at the Northwestern University, USA, from 2016 to 2018. In 2018, he started his independent research career at Northwestern Polytechnical University, China. Currently, his research interests focus on smart lubrication, multifunctional coatings, nanofabrication and optical sensing.

Yong QIAN. He received his bachelor degree in materials science and engineering in 2021 from the University of South China, China, and his master degree in the Center of Advanced Lubrication and Sealing Materials in 2024 from Northwestern Polytechnical University, China. His research interests include studying composite materials based on MOFs and their anti-friction and wear properties.

Feng ZHOU. He is a full professor in Lanzhou Institute of Chemical Physics, Chinese Academy of Sciences, China, and head of Lanzhou Institute of Chemical Physics and State Key Laboratory of Solid Lubrication, China. He gained his Ph.D. degree in 2004 and spent three years (2005–2008) in the Department of Chemistry, University of Cambridge, UK, as a research associate. He has published more than 500 journal papers, which have received more than 28,000 citations and have a high-index of 90. His research interests include bioinspired tribology, biomimic surfaces/interfaces of soft matter, drag-reduction, anti-biofouling, and boundary lubrication.